**Separation Science and Technology**
Publication details, including instructions for authors and subscription information:
http://www.informaworld.com/smpp/title~content=t713708471

# Catalytic Dehydrogenation of Ethanol in Ru-Modified Alumina Membrane Reactor

B. Liu[a]; Y. Cao[a]; J. Deng[a]
[a] DEPARTMENT OF CHEMISTRY, FUDAN UNIVERSITY, SHANGHAI, PEOPLE'S REPUBLIC OF CHINA

**To cite this Article** Liu, B. , Cao, Y. and Deng, J.(1997) 'Catalytic Dehydrogenation of Ethanol in Ru-Modified Alumina Membrane Reactor', Separation Science and Technology, 32: 10, 1683 — 1697
**To link to this Article: DOI:** 10.1080/01496399708000728
**URL:** http://dx.doi.org/10.1080/01496399708000728

SEPARATION SCIENCE AND TECHNOLOGY, **32**(10), pp. 1683–1697, 1997

# Catalytic Dehydrogenation of Ethanol in Ru-Modified Alumina Membrane Reactor

---

BINGSI LIU, YONG CAO, and JINGFA DENG*
DEPARTMENT OF CHEMISTRY
FUDAN UNIVERSITY
SHANGHAI 200433, PEOPLE'S REPUBLIC OF CHINA

## ABSTRACT

Ru-modified alumina composite membranes were prepared by the sol–gel method. The pore size distribution from nitrogen adsorption showed that average pore diameters were 3.1–4.5 nm, and the ideal separation factor was obviously higher than that of a pure $\gamma$-$Al_2O_3$ membrane. Ethanol dehydrogenation was carried out in the Ru-modified alumina membrane reactors. The effects of the reaction temperature, feed rate, and argon sweep flow rate on acetaldehyde yield were investigated. The results showed that the yield of acetaldehyde increased by 25–28% at the same conditions in a Ru-modified alumina membrane reactor. The reduced temperature of the Ru-modified alumina composite membrane was measured by temperature-programmed reduction, and the morphology of the membrane was characterized by SEM, TEM, and XRD.

*Key Words.* Ru-modified alumina membrane; Membrane reactor; Sol–gel method; Ethanol dehydrogenation

## INTRODUCTION

Inorganic membranes have recently attracted extensive interest due to their unique properties such as high thermal and chemical stability, long application life, etc. Much attention has also been paid to ceramic mem-

---

* To whom correspondence should be addressed. Telephone: (+86-21) 65492222 × 3792. FAX: (+86-21) 65490535.

branes for such high-temperature applications as catalytic reaction in a membrane reactor and gas separation at high temperature.

Inorganic membranes can be classified as dense and porous according to their pore structure. Some dense metal membranes have proved to have quite high selectivity for some gases but their permeability is extremely low. On the other hand, porous ceramic membrane have relatively high gas permeability but their separation selectivity is low in general. Therefore, the preparation of inorganic membranes with high selectivity and permeability has been the focus of work by some scientific researchers.

Uhlhorn et al. (1, 2) recently reported that permeation of $CO_2$ and $H_2$ through 17 wt% Ag-containing alumina and silica membranes was promoted by surface diffusion at room temperature. Chai et al. (3, 4) reported that a metal-dispersed mesoporous ceramic membrane could be prepared by adding some metal salts to a boehmite sol which was applied to a membrane reactor for methane steam reformation. The selective permeation of $H_2$ through the membrane was enhanced and, furthermore, the separation factor of $H_2/N_2$ through a metal-dispersed $\gamma$-$Al_2O_3$ membrane exceeded the limitation of the Knudsen diffusion mechanism. Deng et al. (5) reported that Pd and Pt metal particles dispersed in an alumina membrane were effective for promoting hydrogen permeation, and good results for ethanol dehydrogenation incorporating modified membrane reactors were obtained.

In this work we prepared a Ru-modified $\gamma$-$Al_2O_3$ composite membrane by the sol–gel method by introducing fine Ru particles into the microporous structure of an alumina membrane, and we investigated the performance of the membrane reactor through the reaction of ethanol dehydrogenation. The membrane properties were characterized by measuring the microstructure, gas permeability, and separation performance at high temperature.

## EXPERIMENTAL

### Preparation of Ru-Modified $\gamma$-$Al_2O_3$ Composite Membrane

Microporous membranes of alumina were prepared by repeated dip-coating on a porous ceramic tube (average pore diameter 1.1–1.2 μm, porosity 45% O.D. 12 mm, thickness 2 mm, I.D. 8 mm, length 300 mm). The boehmite sol was prepared by a procedure previously described (6). Aluminum isopropoxide, $Al(OC_3H_7)_3$, was dissolved in excess hot water [353 K, $Al(OC_3H_7)_3/H_2O = 0.01$] with vigorous stirring. A clear sol was obtained by introducing dilute HCl [$HCl/Al(OC_3H_7)_3 = 0.1$], increasing the temperature to 363 K, and expelling isopropanol for 4 hours. A solution of $RuCl_3 \cdot xH_2O$ and 1 wt% polyvinyl alcohol were added to the sol. The dip-coated membranes were dried at room temperature for 24 hours and calcined at 753 K for 6 hours following the single dip-coating process. Because the mean pore size of the substrate used in our study is very large (about 1.1–1.2 μm), cracks on the surface of the membrane were easily produced in the process of calcination if a high viscosity Ru-modified boehmite sol was used. The viscosity of the boehmite sol had to be adjusted several times. The dip-coating was repeated 10–15 times. A Ru/$\gamma$-$Al_2O_3$ composite membrane with a thickness of 7–10 μm was prepared.

### Characterization

The Ru-modified $\gamma$-$Al_2O_3$ composite membranes were characterized by scanning electron microscopy (SEM, Hitachi HU-11B STEM), transmission electron microscopy (TEM, H600 STEM), x-ray diffraction (XRD, Regaku Dmax-rA with nickel-filtered CuK$\alpha$ radiation), temperature-programmed reduction (TPR), and nitrogen adsorption (ASAP 2000 adsorption apparatus). A gas permeation test was carried out in a membrane reactor without a catalyst bed. The pure sample gas ($H_2$ or Ar) was introduced into the outer tube and permeated through the membrane into the inner tube. There was a pressure difference (about 40 kPa) between the outer and inner tubes. The amount of permeated gas was measured by a wet flowmeter. The ideal separation factor is defined as

$$\alpha(i/j) = \text{permeability of species } (i)/\text{permeability of species } (j)$$

### Ru/$\gamma$-$Al_2O_3$ Composite Membrane Reactor

The detailed configuration of the Ru-modified $\gamma$-$Al_2O_3$ membrane reactor is shown in Fig. 1. It consists of a glass tube and a Ru-modified $\gamma$-$Al_2O_3$ membrane tube as the outer and inner tubes, respectively. The catalyst was packed in the circular area between the inner and outer tubes. The membrane tube in the catalyst bed kept the gas moving freely. The rest was sealed with heat-resisting adhesive, and both ends of the tubes (i.e., the glass tube and the membrane tube) were fixed with an O-ring seal. Ethanol vapor was carried through the outer path by Ar, where it encountered the catalyst bed packed in the middle of the outer tube. The hydrogen produced from the reaction permeated through the membrane into the inner tube and was carried away by a sweeping argon gas.

### Ethanol Dehydrogenation Using Ru-Modified Membrane Reactor

The ethanol dehydrogenation reaction was carried out in a membrane reactor apparatus shown in Fig. 2. The catalyst used in this study, Cu-P/$SiO_2$ (Cu 2 wt%, Cu/P = 5 mol ratio), prepared by the ion-exchange

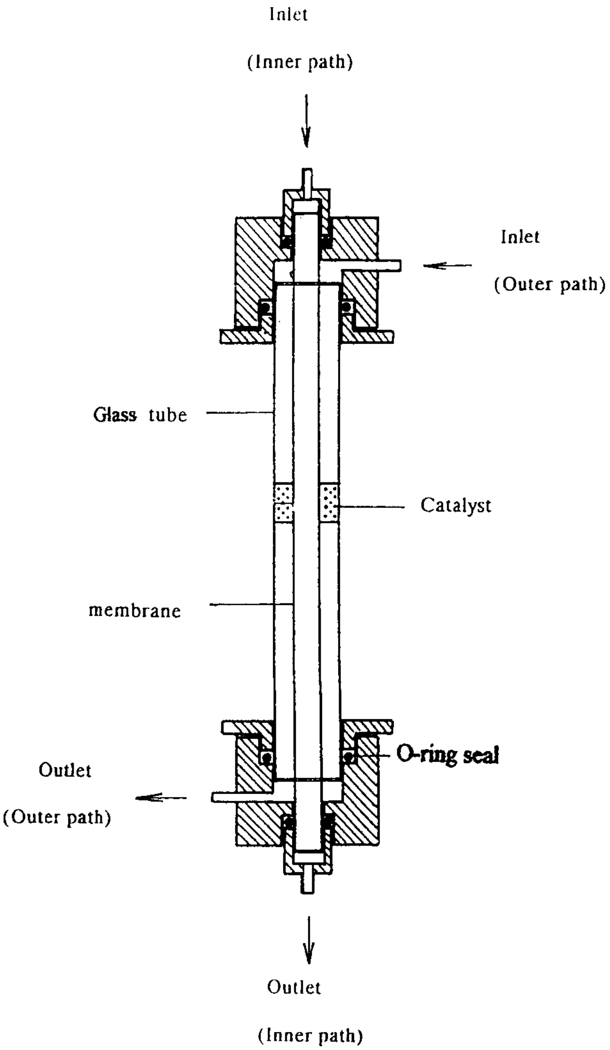

FIG. 1 Ru-modified $\gamma$-$Al_2O_3$ membrane reactor.

method (7, 8), was reduced in a hydrogen flow at 623 K for 2.5 hours before being used in the reaction. The liquid feed (ethanol) was injected at a constant flow rate by a microfeed pump, and it was then vaporized in an evaporator which was kept at a temperature of 120°C. The ethanol vapor was carried by argon gas into the membrane reactor. Meanwhile,

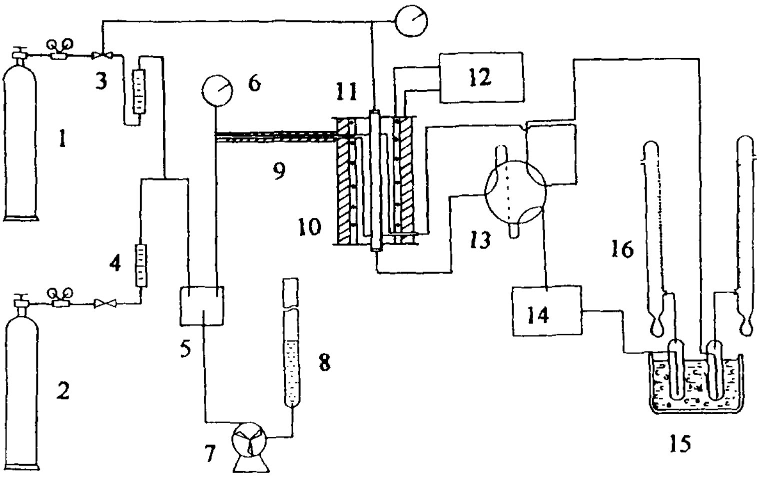

FIG. 2 Schematic diagram of membrane reactor apparatus for ethanol dehydrogenation: (1) Ar gas cylinder, (2) $H_2$ gas cylinder, (3) needle valve, (4) rotary flowmeter, (5) evaporator, (6) pressure gauge, (7) microfeed pump, (8) feed tube, (9) preheating pipe, (10) electric furnace, (11) membrane reactor, (12) temperature controller, (13) six-port valve, (14) 102-gas chromatograph, (15) condensate trap, (16) soap bubble flowmeter.

heating tapes were used to preheat the input stream and prevent condensation in the output stream. The products were analyzed by an on-line gas chromatograph with a thermal conductivity detector (argon was used as the carrier gas, and the column temperature was 145°C), and were also collected in two separate condensate traps. As previously reported (9), the yield of acetaldehyde was calculated according to the following equation:

$$y\% = (W_i y_i + W_o y_o)/(W_i + W_o)$$

where $y_i$ and $y_o$ are the yields of acetaldehyde in the inner and outer tubes, respectively and $W_i$ and $W_o$ are the weights of the condensed products in the inner and outer tubes, respectively

## RESULTS AND DISCUSSION

### Characterization of Ru-Modified Membrane

The isothermal $N_2$ adsorption measurement for the Ru-modified $\gamma$-$Al_2O_3$ membrane illustrated a pore size distribution (Fig. 3). The pore size distribution for the 0.5 wt% Ru-$Al_2O_3$ has a narrow peak around 3 nm, which agrees with the pore distribution for a pure $\gamma$-$Al_2O_3$ membrane (5) prepared

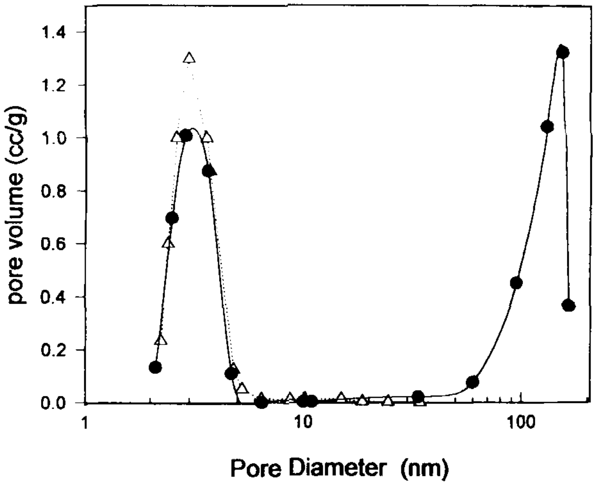

FIG. 3 Pore size distribution curves for Ru-modified alumina membrane: 1.5 wt% Ru-$Al_2O_3$ membrane (●), 0.5 wt% Ru-$Al_2O_3$ membrane (△).

previously, indicating the structural integrity of the membrane. For the 1.5 wt% Ru-modified $\gamma$-$Al_2O_3$ membrane, the pore distribution appeared to have two peaks around 3 and 150 nm. It is suggested that the addition of excess ruthenium resulted in an increase of the pore size of the membrane. This may be due to the enlarged particle size of the sol. Data for the average pore size, pore volume, and specific surface area for the membrane are listed in Table 1.

As shown in Table 1, BET surface area and pore volume gradually declined with an increase of Ru content dispersed in a $\gamma$-$Al_2O_3$ membrane,

TABLE 1
Surface Area, Pore Volume, and Pore Size of Ru-Modified Alumina Membrane

| | Surface area | | Pore volume | | Pore diameter | |
|---|---|---|---|---|---|---|
| Ru-Al membrane | BET ($m^2/g$) | BJH ($m^2/g$) | BET (cc/g) | BJH (cc/g) | BET (nm) | BJH (nm) |
| 1.5 wt% Ru-$Al_2O_3$ | 214.75 | 307.4 | 0.27245 | 0.31072 | 5.1 | 4.0 |
| 0.5 wt% Ru-$Al_2O_3$ | 248.18 | 351.6 | 0.28148 | 0.29705 | 4.5 | 3.4 |
| 0 wt% Ru-$Al_2O_3$ (6) | 274.80 | | 0.30900 | | 3.7 | |

but the pore diameter increased, in accord with the results obtained by Pd and Pt dispersed in a γ-$Al_2O_3$ membrane (5).

The SEM photograph of a Ru-modified alumina composite membrane is shown in Fig. 4. It shows that a crack-free and pinhole-free Ru-$Al_2O_3$ composite membrane was obtained; the thickness of the membrane was about 7–10 μm.

The size of the particles in the membrane layer was investigated by TEM. As shown in Fig. 5, the membrane consisted of fine particles of uniformly deposited Ru metal.

### Temperature-Programmed Reduction Investigation of Ru-Modified Alumina Membrane

The reduction temperature of Ru-modified alumina membrane was investigated by temperature-programmed reduction (TPR). First, a sample of the 1.5 wt% Ru/$Al_2O_3$ composite membrane was heated in flowing $N_2$ at 5 K·min$^{-1}$ to 438 K, held for 30 minutes at 438 K, cooled to room temperature, and then the TPR was carried out, i.e., heating in a 5% $H_2$(Ar) stream at 5 K·min$^{-1}$ to 773 K while the $H_2$ adsorption peak was recorded. Next, $RuO_2$ prepared by treatment of $RuCl_3$ hydrate with air at 101 kPa and 773 K for 40 minutes was taken as a standard sample (only an oxide state, $RuO_2$, confirmed by XPS). The TPR curves are shown in Fig. 6. The alumina boehmite sol containing $RuCl_3$, heated at 773 K,

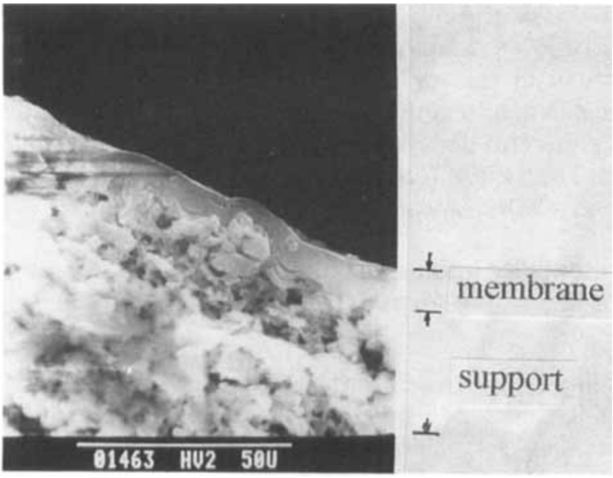

FIG. 4 SEM of the cross section of the Ru-modified alumina membrane.

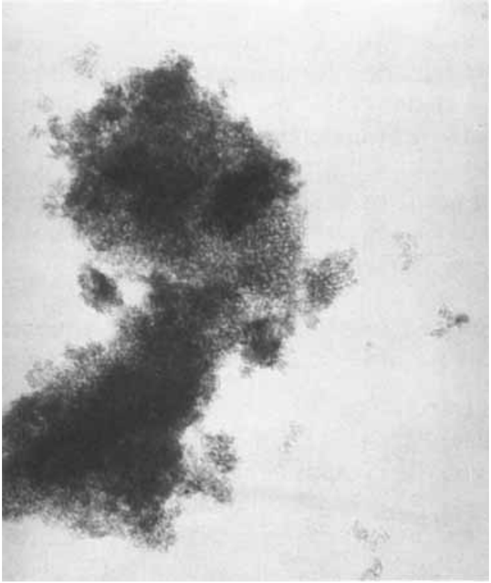

FIG. 5 TEM of the Ru-modified alumina membrane.

appeared to be a $RuO_2/\gamma$-$Al_2O_3$ thin membrane by x-ray diffraction (XRD) analysis (Fig. 7). Therefore, the two reduced peaks in Fig. 6 were assigned to the reduced peak of $RuO_2$. The peak at ~423 K was considered to be the reduction of $RuO_2$, and the other at ~473 K was the reduced peak of the Ru intermediate valence state. It is suggested that the difference in the two curves (a and b) is the result of $RuO_2$ interacting with $\gamma$-$Al_2O_3$.

Koopman et al. (10) directly calcined $RuCl_3/SiO_2$ and obtained $RuO_2/SiO_2$ catalyst. The TPR of $RuO_2/SiO_2$ also showed two peaks at temperature of 450 and 478 K, similar to our experimental results.

## Permeability and Separation Factor of Ru-Modified Alumina Membrane

Figure 8 shows the permeability of $H_2/Ar$ with a change of temperature. The permeability of Ar declined with an increase of temperature according to the law of Knudsen diffusion. But the permeability of hydrogen first decreased and then increased with a rise of temperature. This shows that the permeability of hydrogen is controlled by both surface diffusion and Knudsen diffusion. This is in accordance with Chai's (4) experiment re-

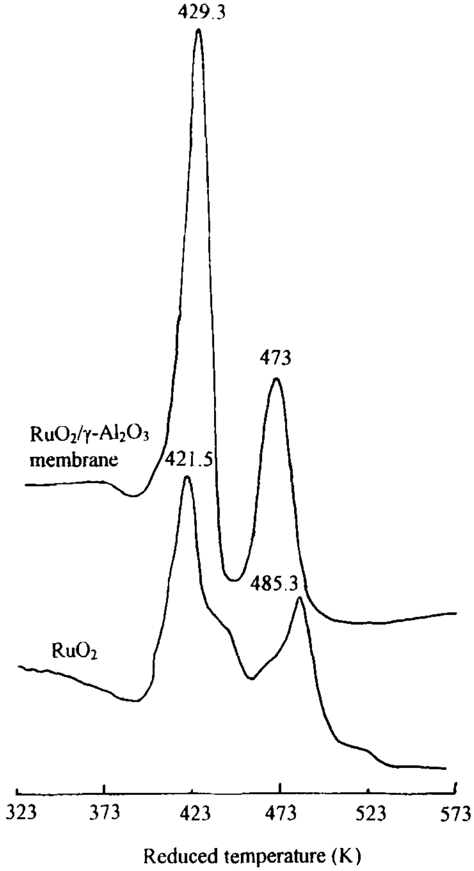

FIG. 6 TPR curves of Ru-modified alumina membrane. (a) $RuO_2/\gamma$-$Al_2O_3$ no loaded membrane. (b) $RuO_2$ obtained by treating $RuCl_3$ hydrate.

sults. Chai et al. proved by $H_2$ adsorption that $H_2$ is chemisorbed on the surface of a metal (like Ru, Pd, Pt) dispersed alumina composite membrane. TPD of $H_2$ on the Rh-$Al_2O_3$ membrane also showed that the high temperature desorption at 400°C can be attributed to spillover of H atoms onto the $Al_2O_3$ support. Therefore, gas diffusion through this membrane is related to $H_2$ chemisorption, desorption of spillover $H_2$ on the surface, and surface diffusion on the wall of the micropores. This further proves the results of our experiments.

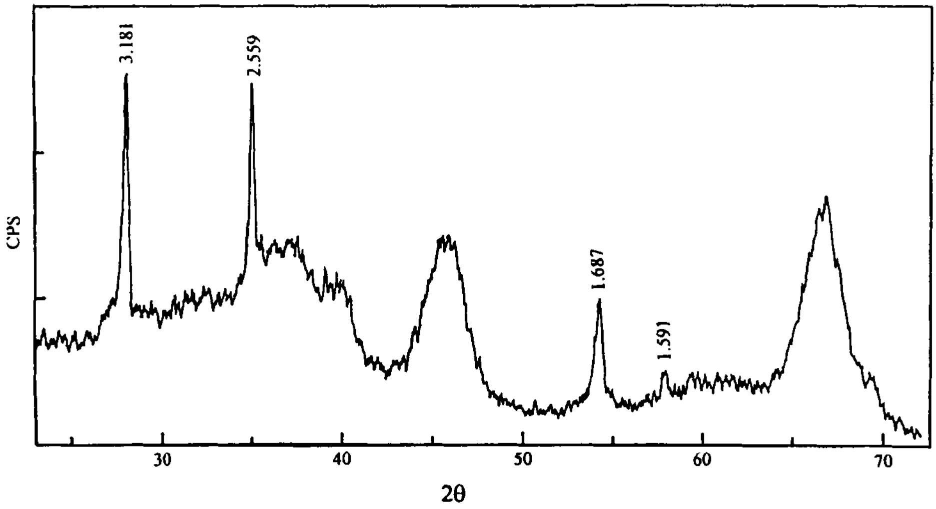

FIG. 7 XRD of 1.5 wt% Ru-modified alumina membrane.

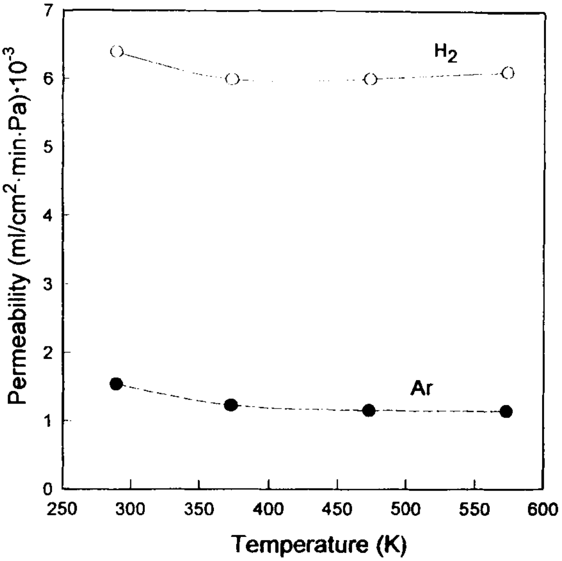

FIG. 8 The effect of temperature on the permeability of $H_2$ (○) and Ar (●).

The ideal separation factor of $H_2/Ar$ with a change of temperature is shown in Fig. 9. For pure $\gamma$-$Al_2O_3$, ideal separation factors nearly approach the Knudsen theoretical value (4.47) at room temperature and then decrease slowly with an increase of temperature. For the Ru-$Al_2O_3$ composite membrane, the separation factor at room temperature was slightly smaller than the theoretical value (4.47) of Knudsen diffusion because of the increased pore diameters. However, it gradually increased with increasing temperature and subsequently far exceeded the Knudsen diffusion value. This shows that the Ru highly dispersed alumina composite membrane had superior adsorbed hydrogen selectivity, indicating the improvement of the separation efficiency of the membrane reactor.

## Catalytic Dehydrogenation of Ethanol Using Ru-Modified Alumina Membrane Reactor

The equilibrium conversion of ethanol dehydrogenation at different temperatures can be calculated on the basis of thermodynamic data (11). Figure 10 shows that the yield of acetaldehyde changed with temperature. For a conventional reactor such as a packed-bed reactor (Fig. 10, Curve

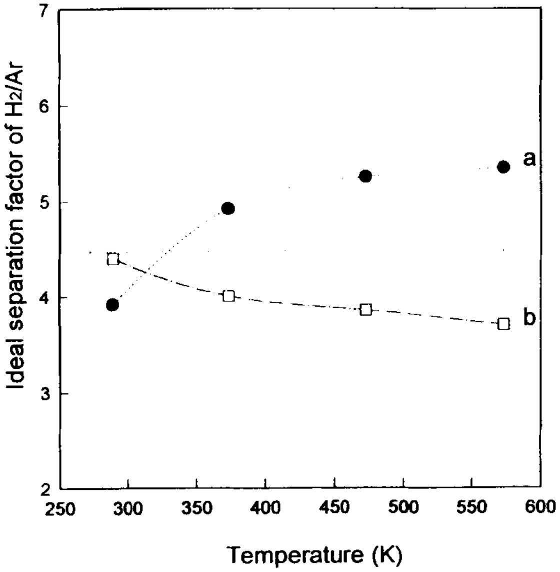

FIG. 9 The effect of temperature on the separation factor of $H_2/Ar$. (a) 0.5 wt% Ru-modified alumina membrane. (b) $\gamma$-$Al_2O_3$ membrane.

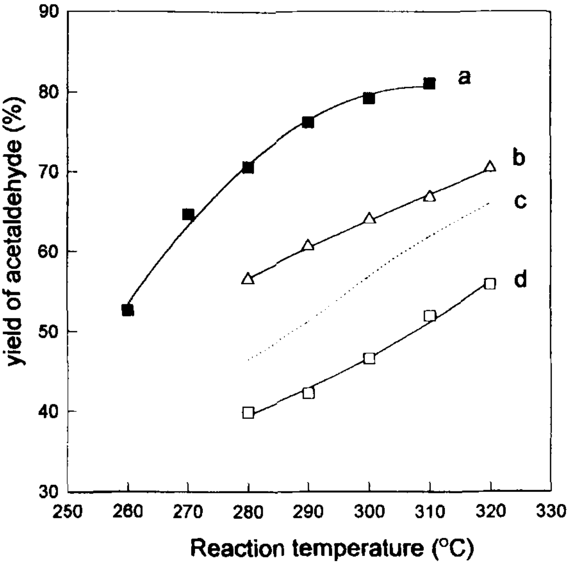

FIG. 10 The effect of reaction temperature on the yield of acetaldehyde. W/F: 1554 gcat·min·mol$^{-1}$; sweeping flow rate: 40 ml·min$^{-1}$. (a) 0.5 wt% Ru-modified alumina membrane reactor, (b) γ-$Al_2O_3$ membrane reactor, (c) equilibrium value, (d) conventional reactor.

d), the yield of acetaldehyde is lower than the corresponding equilibrium yield because of kinetic limitations. For the alumina membrane reactor the hydrogen produced from ethanol diffused to the other side of the membrane by Knudsen diffusion and was carried away by flowing argon. Therefore, the yield of acetaldehyde exceeded the thermodynamic equilibrium value (Fig. 10, Curve b). For the Ru-modified γ-$Al_2O_3$ membrane reactor, the yield of acetaldehyde could be increased by 25–28% under the same conditions and, meanwhile, the selectivity of acetaldehyde nearly reached 100% (not indicated in the figure) at a fair space velocity and with a rationally designed membrane reactor.

For comparison, the dehydrogenation reaction for ethanol was carried out in a Ru-modified alumina membrane reactor without catalyst (Cu-P/$SiO_2$). The yield of acetaldehyde was about 5–7% and didn't increase with an increase of temperature. But this conversion can't simply be compare to that obtained by a membrane reactor with catalyst because when ethanol dehydrogenation was carried out in Ru-modified membrane reactor with catalyst, ethanol vapor first contacted and reacted with the cata-

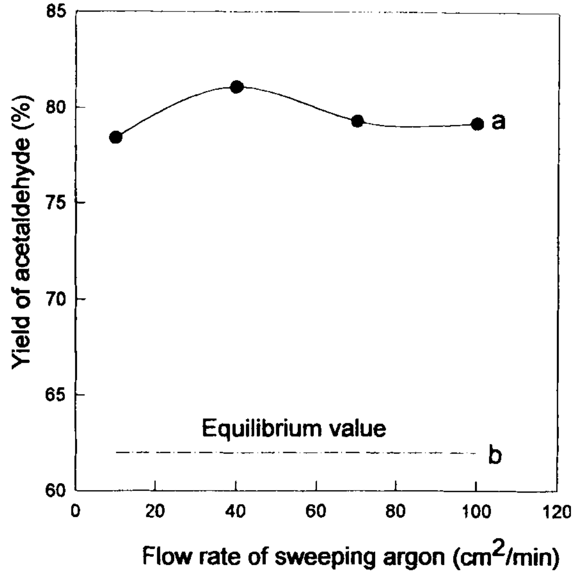

FIG. 11 The effect of the flow rate of sweep Ar on acetaldehyde yield in 0.5 wt% Ru-modified alumina membrane reactor. Reaction temperature: 583 K. W/F: 1554 gcat·min·mol$^{-1}$.

lyst. Hydrogen produced from ethanol was first adsorbed on the surface of the Ru-modified membrane and suppressed ethanol adsorption. Therefore, ethanol concentration on the Ru-modified membrane in this condition was lower than that without catalyst. Therefore, the yield of acetaldehyde must be lower than 5–7%.

Figure 11 shows that the yield of acetaldehyde increases slowly and then gradually declines with an increase of Ar sweeping speed. From the pore distribution and gas permeability of the Ru-modified $\gamma$-$Al_2O_3$ membrane it is known that the Ru-$Al_2O_3$ composite membrane, unlike the dense Pd membrane, not only selectively permeates hydrogen but also partly permeates ethanol and acetaldehyde. Therefore, the permeation of ethanol increases with excessively increasing Ar sweeping speed, and this is partially counteracted by an enhanced acetaldehyde yield.

The effect of the ethanol feed rate on the yield of acetaldehyde is shown in Fig. 12. The acetaldehyde yield increases with increasing space time (W/F) because of the increased contact time of the reactants.

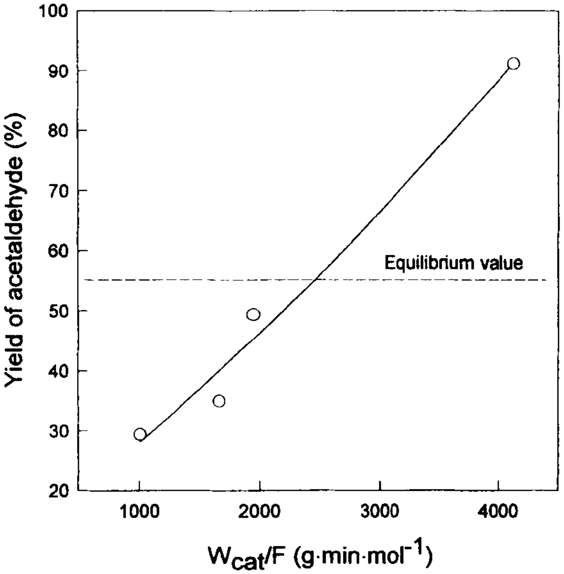

FIG. 12 The effect of space time (W/F) on the yield of acetaldehyde. Reaction temperature: 573 K. Sweeping flow rate: 50 mL·min$^{-1}$.

## CONCLUSION

A Ru/$Al_2O_3$ composite membrane was prepared by the sol–gel method. The ideal separation factor of $H_2$/Ar through the membrane was obviously higher than that of $H_2$/Ar through a $\gamma$-$Al_2O_3$ membrane. Ru particles were found to be highly dispersed in the $\gamma$-$Al_2O_3$ membrane.

Ethanol dehydrogenation was carried out in Ru-modified alumina composite membrane reactors. The yield of acetaldehyde was much higher than that in inorganic $\gamma$-$Al_2O_3$ membranes and in Pd and Pt dispersed alumina composite membrane reactors (5) due to the particular hydrogen absorbility of Ru metal.

## REFERENCES

1. R. J. R. Uhlhon, K. Keizer, and A. J. Burggraaf, *J. Membr. Sci.*, *46*, 225 (1989).
2. R. J. R. Uhlhon, M. H. B. J. Huisin't Veld, K. Keizer, and A. J. Burggraaf, *J. Mater. Sci. Lett.*, *8*, 1135 (1989).
3. M. Chai. M. Machida, K. Eguchi, and H. Arai, *Appl. Catal.*, *110*, 239 (1994).

4. M. Chai, Y. Yamashite, M. Machida, K. Eguchi, and H. Arai, *J. Membr. Sci.*, *97*, 199 (1994).
5. Jingfa Deng, Zhao Cao, and Bo Zhou, *Appl. Catal.*, *132*, 9 (1995).
6. Zhao Cao and Jingfa Deng, *Chem. J. Chin. Univ.*, *14*(11), 1593 (1993).
7. T. Sodcsawa, M. Nagacho, A. Onodera, and F. Nozaki, *J. Catal.*, *102*, 460 (1986).
8. T. Yamamoto, A. Shimoda, T. Okuhara, and M. Misono, *Chem. Lett.*, p. 273 (1988).
9. Jingfa Deng and Jingtao Wu, *Appl. Catal.*, *109*, 63 (1994).
10. P. G. J. Koopman, A. P. G. Kieboom, and H. Van Bekkum, *J. Catal.*, *69*, 172 (1981).
11. Yongja Yin, *Wuli Huaxue Jianming Shouce*, Beijing Higher Education Press, Beijing, 1986, p. 76.

*Received by editor May 29, 1996*
*First revision received September 1996*
*Second revision received November 1996*